Wiesand, U., Sorg, I., Amstutz, M., Wagner, S., van den Heuvel, J., Lührs, T., Cornelis, G.R., Heinz, D.W.
Structure of the Type III Secretion Recognition Protein YscU from Yersinia enterocolitica
(2009) Journal of Molecular Biology, 385 (3), pp. 854-866.

Structure of the type III secretion recognition protein YscU from *Yersinia enterocolitica*

Ulrich Wiesand[1], Isabel Sorg[2], Marlise Amstutz[2], Stefanie Wagner[2], Joop van den Heuvel[1], Thorsten Lührs[1], Guy R. Cornelis[2], and Dirk W. Heinz[1*]

[1]Division of Structural Biology, Helmholtz Centre for Infection Research (HZI), Inhoffenstrasse 7, 38124 Braunschweig, Germany

[2] Division of Molecular Microbiology, Biozentrum, University of Basel, Klingelbergstrasse 50/70, CH-4056 Basel, Switzerland

Running title: Structure of YscU

*Corresponding author:
Division of Structural Biology
Helmholtz Centre for Infection Research, Inhoffenstrasse 7, D-38124 Braunschweig, Germany
Phone: +49-531-6181-7000, Email: Dirk.Heinz@helmholtz-hzi.de

Keywords:
auto-proteolysis, crystal structure, translocators, type III secretion system, *Yersinia*

Abbreviations:
$YscU^C$ = C-terminal domain of YscU comprising amino acids 211-354
T3SS = type III secretion system

Abstract

The inner-membrane protein YscU has an important role during the assembly of the *Yersinia enterocolitica* type III secretion injectisome. Its cytoplasmic domain ($YscU^C$) recognizes translocators as individual substrates in the export hierarchy. Activation of YscU entails autocleavage at a conserved NPTH motif. Modification of this motif markedly changes the properties of YscU including translocator export cessation and production of longer injectisome needles.

We determined the crystal structures of the uncleaved variants N263A and N263D of $YscU^C$ at 2.05 Å and 1.55 Å resolution, respectively. The globular domain is found to consist of a central, mixed β-sheet surrounded by α-helices. The NPTH motif forms a type II β-turn connecting two β-strands. NMR analysis of cleaved and uncleaved $YscU^C$ indicates that the global structure of the protein is retained in cleaved $YscU^C$. The structure of $YscU^C$ variant N263D reveals that wild-type $YscU^C$ is poised for cleavage due to an optimal reaction geometry for nucleophilic attack of the scissile bond by the side-chain of Asn263. I*n vivo* analysis of N263Q and H266A/R314A YscU variants showed a phenotype that combines the absence of translocator secretion with normal needle-length control. Comparing the structure of YscU to those of related proteins reveals that the linker domain between the N-terminal transmembrane domain and the autocleavage domain can switch from an extended to a largely α-helical conformation, allowing for optimal positioning of the autocleavage domain during injectisome assembly.

Introduction

The enteric pathogen *Yersinia enterocolitica* uses a sophisticated injection machinery called an injectisome to translocate effector proteins across eukaryotic cell membranes by type III secretion (T3S). This supramolecular structure, found in many Gram-negative pathogenic or symbiotic bacteria, including *Salmonella* spp., *Shigella* spp. and enteropathogenic *Escherichia coli*, is evolutionarily related to the bacterial flagellum.[1] A basal body consisting of several rings connected by a central rod spans the two bacterial membranes in both structures.[2-5] The basal body bears an extracellular structure referred to as a needle[2,3,6-8], pilus[9] or filament,[10-12] depending on the family of injectisomes. Upon contact with the eukaryotic host cell, a set of effector proteins that subvert host cellular functions to the pathogen`s benefit is translocated into the eukaryotic cytoplasm.[13,14]

The rotationally symmetric basal body of the T3S system (T3SS) actively exports the components of the extracellular needle structure.[3,4,15,16] The length of the *Yersinia* injectisome needle, assembled from the 9-kDa protein YscF, differs from species to species. In *Yersinia enterocolitica,* the needle length of ~60 nm correlates with the length of the “molecular ruler” protein YscP.[17] A needle tip complex, made of the protein LcrV,[18] functions as a scaffold to assemble a pore in the target cell membrane consisting of YopB and YopD, through which T3SS effectors are translocated into the host cell.[19] Beside the “molecular ruler” model,[14] two other models for needle/hook length control, the cup model[20] and the molecular stopwatch mechanism,[21] are discussed. As a clear hierarchy in the synthesis of the needle components is not discernible, the T3SS presumably discriminates between substrate classes to assemble this complex molecular machine.[22] Needle assembly depends on the export of early substrates such as the needle subunit YscF and the molecular ruler YscP. Thereafter, the system switches its substrate specificity to intermediate (translocators) and late (effectors) export substrates. The substrate specificity switch is thought to involve at least two proteins, the molecular ruler YscP and the inner membrane protein YscU.[23,24]

In the 40 kDa membrane protein YscU, four N-terminal transmembrane helices are followed by a globular cytoplasmic domain ($YscU^C$).[25] The latter, which was originally been found in the C-terminal cytoplasmic domain of the *Salmonella* flagellar YscU homolog, FlhB,[26] is cleaved autoproteolytically within a conserved NPTH sequence.[27]

Autocleavage, however, is abrogated by substituting either asparagine or proline by alanine.[27] Bacterial mutants carrying these substitutions no longer export translocator proteins (YopB, YopD and LcrV), whereas export of effector proteins is not affected.[22] Cleaved YscU thus appears to discriminate between translocator and effector proteins. The mutant *yscU*$_{N263A}$, furthermore, secretes less YscP and makes longer needles.[22]

Here, we report the crystal structures of the non-cleavable YscU$^{C}_{N263A}$ and YscU$^{C}_{N263D}$ variants from *Yersinia enterocolitica* and compare them to the related structures of EscU, SpaS[28] and Spa40.[29] Based on the structural information, additional YscU^{C} mutants were designed to elucidate their *in vitro* autocleavage behaviour and the nature of the resulting *in vivo* phenotypes.

Results

Crystal structures of YscU^C N263A and N263D

The YscU^C variants N263A and N263D readily yielded well-diffracting tetragonal crystals. Crystallization of cleaved, wild type YscU^C, by contrast, was not successful. The structure of YscU^C N263A was solved using SeMet-based multiwavelenght anomalous diffraction (MAD) phasing. Two (of four expected) selenium positions were sufficient to build an initial model, which was refined at a resolution of 2.05 Å (Table 1). The isomorphous structure of YscU^C N263D was correspondingly refined at a resolution of 1.55 Å (Table 1).

Tab. 1

Fig. 1

The globular domain of uncleaved YscU^C (Fig. 1) consists of a central, five-stranded, mixed β-sheet (I-V), surrounded by four α-helices (1-4). α-helix 3 is almost perpendicular to the strand orientation of the central β-sheet. The NPTH-cleavage motif forms a type II β-turn connecting β-strands I and II with position 263 located at the C-terminal end of β-strand I.

The globular autocleavage domain is preceded by an extended N-terminal loop containing a well defined α-helix (α0) comprising residues 232-244. This helix forms an antiparallel interaction with helix 4 of a symmetry-related YscU^C monomer in the crystal.

Structural basis for autocleavage of YscU

Close inspection of the modified NPTH motif in isosteric variant YscU^C N263D (DPTH, Fig. 2a) shows that the main-chain carbonyl of Asp263 is tightly locked into position *via* hydrogen bonds to the backbone nitrogen atoms of His266 and Ile267. This structural stiffness is enhanced by the peptide bond of Pro264. All main-chain dihedral angles of the DPTH residues fall in the allowed regions of the Ramachandran plot, indicating no obvious conformational strain. A salt bridge with the guanidinium group of Arg314 positions the side chain of Asp263 above its main-chain carbonyl group.

Fig. 2

The ideal entry angle for a nucleophilic attack of a carbonyl group has been proposed to lie between 100° and 110°, and a distance between nucleophile and electrophile of 2.5 Å. [30,31] The corresponding angle of the YscU^C N263D variant is 109° with an N-C distance of 2.8 Å. The β-amide nitrogen of Asn263 would therefore be positioned perfectly for a nucleophilic attack. Furthermore this geometric arrangement favours a stabilizing orbital overlap (Fig. 2b), where the anti-binding σ*-molecular orbital (MO) of

the $C_{\alpha Asn}$-N_{Asn} bond interferes with the nascent binding σ-MO of the C(=O)-N-bond in native YscU.

Cleavage does not affect the overall structure of wild-type YscU^C

Recombinantly produced wild-type YscU^C is readily cleaved into a ~ 6.3 kDa N-terminal (α-helices 0-1 and β-strand I) and a ~10.5 kDa C-terminal (α-helices 2-4 and β-strands II-V) fragment. The fragments, remain tightly linked, however,[27] resulting in a single peak in gel-filtration chromatography (data not shown). Cleavage of the wild-type protein thus does not cause significant overall structural rearrangements compared to the uncleaved YscU^C variants. This was confirmed by 2D-NMR ([^{15}N,^{1}H]-HMQC) spectroscopy by comparing ^{15}N-labelled wild-type and N263A YscU^C (Fig. 3). Overall, wild-type YscU^C shows a good dispersion of the signals, characteristic for a folded globular conformation. An equally good dispersion of the signals is observed for N263A YscU^C. The NMR-spectra of wild-type and N263A YscU^C superimpose very well, with most peak positions being are virtually identical and line-widths apparently unaffected. Cleaved and uncleaved YscU thus share the same overall structure with minor, but physiologically highly relevant, changes in and close to the NPTH motif.

Fig. 3

The role of conserved amino acids in YscU^C cleavage in vitro

Substituting the nucleophile Asn263 by alanine, aspartate and glutamine abolishes autocleavage of YscU. While Asn263 is thus essential for YscU–autocleavage, the role of surrounding residues is less clear. A systematic mutational analysis of the NPTH motif reveals an active participation of Pro264 and His266 in YscU autocleavage (Fig. 4a and b), whereas Thr265 is not involved.[22] Substitution of Pro264 by alanine reduces cleavage of YscU^C significantly, whereas substitution by glycine prevents cleavage altogether. Variant H266A shows a partial cleavage of YscU^C. The structure of YscU^C shows that two arginine residues (Arg296 and 314) flank the NPTH motif. Of these, Arg314 is highly conserved, Arg296 less so. Substituting Arg314 by alanine correspondingly reduces cleavage partly whereas cleavage of variant R296A is unaffected. Interestingly, cleavage is entirely abrogated in the double variant H266A/R314A, suggesting a synergistic involvement of these residues in the mechanism of cleavage.

Fig. 4

Cleavage of some autocleavage-deficient YscU mutants is partially restored at high pH

Autocleavage of the slow-cleaving variant P270A of the flagellar protein $FlhB^C$ (a homologue of $YscU^C$) has previously been reported to be pH-dependent[32]. $YscU^C$ variants N263D, P264G, P264A and H266A/R314A were therefore analysed at pH 9, 10 and 11 (Fig. 4c). In variant N263D, no cleavage was observed at higher pH-values, whereas P264G, P264A and H266A/R314A were partially cleaved only at elevated pH. These observations match the published data on FlhB P270A,[32] suggesting that the nucleophile Asn263 needs to be activated by deprotonation of its side chain amide group.

Fig. 4

YscU mutants that are not cleaved *in vitro* do not export the translocator LcrV

Next, the export of the LcrV protein in the corresponding *Yersinia* mutant strains was investigated. Secretion was not affected for wild-type YscU, and the variants H266A, R314A and R296A, but is lost in variants N263A, N263D, N263Q, P264A, P264G, and H266A/R314A, as confirmed by an immunoblot of the supernatant (Fig. 5). The LcrV secretion pattern is in excellent agreement with the data described above for *in vitro* autocleavage.

Fig. 5

The T3SS injectisome needle length is influenced strongly by YscU mutations

The influence of the YscU modifications on needle length was investigated by measuring needles from *Y. enterocolitica* Δ*yscU* mutant bacteria expressing the respective mutants in *trans*. Bacteria expressing wild-type *yscU* produced regulated needles of 69±10 nm. Similar needle lengths were measured for the YscU variants H266A (67±9nm), R314A (72±12nm), and R296A (76±11nm). In contrast, the length of needles in YscU variants N263A (125±40nm), N263D (143±51nm), P264A (112±42nm), and P264G (114±30nm) was longer and less regulated. Interestingly, YscU variants N263Q (80±16nm) and H266A/R314A (77±15nm) were regulated with a length distribution slightly larger than that of wild-type YscU (Fig. 6).

Fig. 6

Discussion

YscU is poised for autocatalytic cleavage

To elucidate the structural basis of $YscU^C$ autocleavage, the crystal structures of $YscU^C$ variants N263A and N263D were determined at high resolution. Additional single-residue $YscU^C$ variants within the NPTH motif or its immediate vicinity were investigated with respect to their participation in cleavage and needle-length control.

The crystal structure of non-cleaving $YscU^C$ variant N263D (the asparagine nucleophile is replaced by the isosteric homologue aspartate) suggests that the side-chain of Asn263 is positioned ideally for a nucleophilic attack and subsequent cleavage of wild-type $YscU^C$. In N263D, the attack on its own carbonyl is prevented by the insufficient nucleophilicity of the Asp 263 carboxylate, despite its equivalent positioning. In N263Q, the nucleophilicity should be similar to that of asparagine. However, the longer and hence more flexible, side chain disfavours the formation of a lactam ring in this variant, preventing cleavage of $YscU^C$.

$YscU^C$ autocleavage is crucially dependent on the positioning of the attacked carbonyl group of Asn263, which is part of the peptide bond to Pro264. Increased flexibility of the main chain correspondingly disfavours cleavage in the variants P264A and P264G. As indicated above, cleavage is less efficient in variants H266A and R314A, but entirely abrogated in H266A/R314A. Increasing the pH increases cleavage, implicating both His266 and Arg314 in efficient autocleavage. By means of a hydrogen bond, Arg314 presumably serves to optimally position the side chain of Asn263 allowing nucleophilic attack to occur at an angle of 109°. The role of His266 is, however, less clear. It may potentially mediate the abstraction of a proton from Asn263 either directly or by deprotonating an intermediate water molecule. A similar phenomenon has been proposed for a histidine residue during autosplicing of the DnaB mini-intein.[33] Thr265, as the only imperfectly conserved amino acid of the NPTH motif, does not appear to be involved directly in the cleavage reaction.[22,28] A preference for β-branched amino acids indicates a role in stabilizing the type II turn.[34]

Our results are supported by similar structural and functional data recently reported for the YscU homologues EscU from enteropatogenic *E. coli*, SpaS from *Salmonella typhimurium*[28] and Spa40 from *Shigella Flexneri.*[29] The crystal structures of the cleaved wild type EscU as well as a number of EscU variants were determined and

correlated with *in vivo* cleavage experiments of full-length EscU (variants). Wild type EscU, SpaS and Spa40 reveal unchanged tertiary structures of nicked proteins, concurring with our conclusion based on NMR-analysis of $YscU^C$ wild type and mutant. The only major differences concern $YscU^C$ variants H266A and R314A and their homologous variants *in vivo* in full-length EscU. Both $YscU^C$ variants show partial autocleavage *in vitro* and a wild type-like secretion of LcrV *in vivo*. EscU variant H265A is found be fully autocleaved but secretion of T3S substrates is lost[28]. EscU variant R313A, by contrast, remains uncleaved but again T3S substrates secretion is lost.[28] A third EscU variant, R133T, is fully cleaved but retains normal effector secretion.[28] Thus, despite a high level of structural conservation between YscU and EscU, some differences between the *Yersina* and EPEC T3SS may exist. The *in vitro* cleavage data on $YscU^C$ His266 variants would presumably implicate His265 in EscU in the asparagine-driven autocleavage reaction.

Fig. 7

We propose the following autocleavage reaction mechanism (Fig. 7). (i) The unique reaction geometry of YscU and its homologues is a prerequiste for the nucleophilic attack. The β-amide nitrogen, activated through proton abstraction by His266 or an intermediate water molecule, is optimally positioned to attack the electrophilic carbonyl carbon at an angle of 109° (108° in EscU). (ii) The tetrahedral reaction intermediate is stabilized by hydrogen bonds to the backbone amides of His266 and Ile267. (iii) Protein cleavage gives rise to a labile succinimide, which is rapidly hydrolysed to yield a new C-terminal asparagine or iso-asparagine.

The structure of $YscU^C$ also explains phenotypes of previously reported YscU variants. The strongly reduced export of the presumed inner rod protein YscI (in an *yscPyscU* mutant background) in the YscU variant Y317D implicates Tyr317 in interacting directly with YscI.[35] Structurally, this strictly conserved residue is fully exposed at the surface of α-helix 3. Presumably, the introduction of a negative charge prevents interaction with YscI explaining the observed phenotype.[28] The YscU variant G270N has been reported to cause the complete loss of T3S and YscU autocleavage.[36] Gly270, in the middle in β-strand II, is fully buried in the hydrophobic core of the domain. Replacing this by the significantly bulkier asparagine presumably prevents correct protein folding, resulting in the loss of this protein and non-functional T3SS.

Needle length in a non-cleavable YscU mutant is controlled even without YscP over-expression

In vivo analyses reveal a new phenotype for the YscU variants N263Q and H266A/R314A. These variants do not undergo autocleavage *in vitro*. Corresponding bacterial mutants do not secrete the translocator LcrV. Their needles are, however, of normal size, although significantly less YscP is secreted compared to wild type bacteria (data not shown). In the YscU N263A mutant, wild type needle length could be restored only by YscP over-expression implying that YscU autocleavage inhibition diminishes YscP secretion losing control over needle length.[22] The phenotype observed here for the variants N263Q and H266A/R314A demonstrates that the inhibition of the autocleavage may indeed affect the secretion of YscP and LcrV without relinquishing control over needle length. The fact that different phenotypes are observed for N263A and N263Q despite involving the same residue, may indicate that small amounts of YscP are sufficient to determine needle length but that a defined conformation of YscU is also required.

The flexible linker region is composed of two hinged α-helices

Fig. 8

A structural superposition of uncleaved $YscU^C$ variant N263A with $EscU^C$ (rmsd 1.3 Å for 94 common Cα atoms), SpaS form *Salmonella typhimurium* (rmsd 1.0 Å for 80 Cα atoms), and Spa40 from *Shigella flexneri* (rmsd 1.0 Å for 82 Cα atoms) reveal virtually identical folds for the cytoplasmic core region and the NPTH motifs (Fig. 8b), despite a low level of overall sequence identity (Fig. 8a).

An obvious difference between $YscU^C$ and its homologues $EscU^C$, $SpaS^C$ and $Spa40^C$ involves the proposed flexible linker (211-248) connecting the globular autocleavage domain to the N-terminal membrane-spanning four-helix bundle (Fig. 8b). In $YscU^C$, amino acids 232-244 form a well-defined α-helix, which is not observed in the homologous structures. In the crystal structure of $YscU^C$, α-helix α0 is involved in a crystal contact to α-helix α4 of the next monomer. One of the crystal forms of $EscU^C$ additionally reveals a further α-helix (α-1) N-terminal of α0.[28]The presence of α-helix α0 confirms earlier predictions of the secondary structure for the flagellar protein FlhB.[37]

The linker region is essential for T3S.[28] Corresponding deletions 232-236, 234-245 and 230-245 in EscU and the point mutation G235P (S236P in YscU) abolish the export of T3S substrates, despite autocleavage of EscU being detectable. Similar

results have been obtained for the FlhB protein.[37] Mapping these mutations onto the structure of $YscU^C$ indicates that each would delete or kink α-helix α0, which presumably functions as a spacer element, separating the globular autocleavage domain from the inner membrane. Additionally, the helix could be involved in direct or indirect binding of other components.

Amino acids such as Gly229 and Gly248 in EscU are assumed to provide flexibility to the linker region.[28] Substituting conserved Gly229 by proline in EscU (G230 in YscU and located N-terminal of α-helix α0) decrease the export of T3S substrates dramatically. An equivalent substitution in Gly247 (G248P in YscU and located C-terminal of α0) also reduces the export of T3S substrates. Combining the structural information on $YscU^C$ and $EscU^C$ with the *in vivo* data suggests that YscU-like proteins are composed of three units (Fig. 9): A membrane-spanning N-terminal domain and a C-terminal, cytoplasmic, globular, autocleavage domain bridged by a flexible linker region that can switch from an extended to a partially α-helical conformation. This adaptable architecture of the linker allows for sufficent conformational freedom to enable interactions of the autocleavage domain with other components of the T3SS during T3SS assembly.

Fig. 9

Acknowledgements

We thank Hauke Pagel for his support during the initial stage of protein preparation. We are also grateful to Dr. Manfred Weiss (DESY/ EMBL, beamline X12), the team of ESRF-ID29, for helping during data collection and processing and to Dr. Victor Wray and Dr. Wolf-Dieter Schubert for critical comments on the manuscript. D.W.H. acknowledges support by the Fonds der Chemischen Industrie. This work was supported by the Swiss National Science Foundation (grant 310000 – 113333/1 to GRC).

Materials and Methods

YscU in vivo experiments

Supp. 1

Bacterial strains, plasmids and genetic constructions are given in Supplementary Data Table 1. *E. coli* Top10 was used for plasmid purification and cloning. Bacteria were grown routinely on Luria-Bertani (LB) agar plates and in liquid LB-medium. Ampicillin was used at concentrations of 200 µg/ml.

Supp. 2

Plasmids were generated using either the *Pfu* turbo polymerase (Stratagene) or Vent DNA polymerase (New England, Biolabs). Oligonucleotides for genetic constructs are given in Supplementary Data Table 2. All constructs were confirmed by sequencing using a 3100-Avant genetic analyser (ABI Prism).

LcrV secretion and immunoblotting

Induction of the *yop* regulon was as described by Cornelis *et al.*.[38] Expression of the different genes cloned downstream of the pBAD promoter was induced routinely by adding 0.2 % L-arabinose to the culture before the shift to 37 °C, and again 2 hours later. Glycerol (4 mg/ml) was added as a carbon source when expressing genes from the pBAD promoter. Total cell and supernatant fractions were separated by centrifugation at 20,800*g* for 10 min at 4 °C. The cell pellet was taken as the total cell fraction. Proteins in the supernatant were precipitated with 10 % (w/v) trichloroacetic acid (final concentration) for 1 hour at 4 °C.

Supernatant (SN) and total cell (TC) fractions were separated bay SDS/12% PAGE. In each case, proteins secreted (SN) or produced (TC) by 2.5 x 10^7 bacteria were loaded in each lane. Immunoblotting was done using rabbit polyclonal antibodies against LcrV (MIPA220; 1:2000). Detection was done with the respective secondary antibodies conjugated to horseradish peroxidase (1:5000; Dako), before development with supersignal chemiluminescent substrate (Pierce).

Electron microscopy

Needles were visualized by transmission electron microscopy as described.[8,23]. After induction of the *yop* regulon for 4 h at 37 °C bacteria were harvested by centrifugation at 2000*g* and resuspended gently in 20 mM Tris-HCl, pH 7.5. Droplets were applied for 1 minute to freshly glow-discharged, formvar-carbon coated grids, and negatively stained with 2 % (w/v) uranyl acetate. Bacteria were visualized in a Philips CM100

transmission electron microscope at a nominal magnification of 20,000*x* and an acceleration voltage of 80 kV. Sizes were measured with the Soft imaging system software (Hamburg, Germany).

Expression and Purification of YscU^C

The cytoplasmic domain of YscU^C was expressed in *E.coli* Tuner (DE3) cells using vector pGEX-6P-1 (GE Healthcare). A single colony was used to inoculate a preculture of 20 mL of Luria-Bertani medium with 200 µg/mL of ampicillin. The cells were grown at 37 °C to an A_{600} of 0.6. A 10 mL preculture was transferred in 1 L of Terrific Broth (100 µg/mL of ampicillin), grown at 37 °C to an A_{600} of 0.6, supplemented with 0.2 mM isopropyl thiogalactopyranoside, incubated for 16 h, and then harvested by centrifugation.

Harvested cells were resuspended in PBS, containing 2 µL of Benzonase (250 U/mL, Novagen) and 1 tablet of Complete Mini Protease Inhibitor (Roche). Cells were lysed by French press and centrifuged. The supernant was incubated with glutathione Sepharose (GS, GE Healthcare) for 4 h at 4 °C. Unbound protein was washed three times from the GS column with protease buffer (50 mM Trizma base pH 7.5, 150 mM NaCl, 1 mM DTT, 1 mM EDTA). A 75 µL sample of PreScission Protease (GE Healthcare) in 10 mL protease buffer was incubated with loaded GS over night at 4 °C. The protein was eluted four times with protease buffer and dialysed against buffer A (20 mM Hepes, pH 7.0, 100 mM NaCl). The protein solution was applied to a cation-exchange column (MonoS, GE Healthcare) equilibrated with buffer A and eluted with a 0.1 M -1 M NaCl gradient in buffer A. The YscU^C-containing fractions were identified by SDS-PAGE, concentrated to 5 -15 mg/mL and further purified using a gel permeation column (Superdex S75 16/60, GE Healthcare) equilibrated with 20 mM Hepes pH 7.0, 150 mM NaCl. L-Selenomethionine (SeMet)-labelled and ^{15}N-labelled YscU^C N263A, as well as ^{15}N-labelled YscU^C wild type were as described.[39] YscU^C mutations were introduced using the QuikChange kit (Stratagene) and verified by DNA sequencing (GATC, Konstanz, Germany). YscU^C variants were purified as described above.

Preparation of pH-dependet cleavage

The different YscU^C variants were expressed and purified as described above. P264A was dialysed against 25 mM Ches-buffer, 100 mM NaCl for 3h at room temperature.

P624G, H266A/R314A and N263D were dialysed against 25 mM CAPS-buffer, 100 mM NaCl for 4h at room temperature. Afterwards, the solution of protein P264G was stored for 48 h and H266A/R314A and N263D were stored for 24 h at 4 °C. Cleaved proteins were submitted to SDS/15% PAGE and stained with Coomassie brilliant blue.

Crystallization and Structure Determination

$YscU^C$ N263A and its SeMet-labelled derivative were crystallised using the hanging drop method using 3 µL of a 8 mg/mL protein solution mixed with 3 µL of reservoir buffer (1.6 M $(NH_4)_2SO_4$, 0.2 M NaCl, 0.1 M Hepes, pH 7.5) in the droplet. Crystals grew within ~4 days at 20 °C to sizes of up to 180 µm x 180 µm x 120 µm. Crystals were transferred in cryo buffer containing reservoir buffer with 16 % (v/v) glycerol as a cryo protectant and flash-frozen at 100 K in liquid nitrogen. Four multiwavelength anomalous diffraction (MAD) data sets of SeMet-labelled $YscU^C$ N263A were collected at beamline X12 at the EMBL Outstation (Hamburg, Germany) and processed with the HKL2000[40] and MOSFLM.[41] Localization of two selenium sites, which were used for phasing and the generation of a partial model, was done with AUTORICKSHAW.[42] Manual model building was carried out using COOT[43] and refinement was completed using REFMAC5. [44]

The X-ray data set of $YscU^C$ N263D was collected at ESRF beamline ID29 (Grenoble, France), processed with MOSFLM[41] and scaled with SCALA.[45] Using REFMAC5[46] and SeMet-labelled $YscU^C$ N263A as a phasing model, the structure was solved by difference fourier and further refined with COOT [43] and REFMAC5.[44]

The validation of both structures was done with MOLPROBITY.[47] Data collection and refinement statistics are given in Table 1. Figures were prepared using PYMOL (http://pymol.org).

Tab. 1

NMR Analysis

For NMR spectroscopy, we used a 12 mg/mL solution of uniformly ^{15}N-labelled $YscU^C$ in a mixed solvent of 95% (v/v) H_2O, 5% (v/v) ^2H_2O and a 10 mg/mL solution of $YscU^C$ N263A in the same solvent. The NMR samples contained 50 mM NaCl, 3 mM KCl, 12 mM Na_2HPO_4 and 2 mM KH_2PO_4 at pH 6.8. The Bruker Advance III 600 spectrometer used for this study was equipped with a 5-mm Z-axis gradient triple-resonance cryo-probehead. The 2D [^{15}N,^1H] correlation spectra were recorded at

ω_1 = 2100 Hz and ω_1 = 8400 Hz. The maximal evolution times were t_{1max} = 60 ms and t_{2max} = 240 ms and the time domain data size was 256 × 2048. Programs PROSA[48] and CARA[49] were used for data processing and spectral analysis, respectively.

Protein Data bank accession codes

The coordinates have been deposited in the Protein Data bank (PDB) under accession code 2v5g and 2w0r.

References

1. Macnab, R. M. (2003). How bacteria assemble flagella. *Annu Rev Microbiol* **57**, 77-100.

2. Blocker, A., Gounon, P., Larquet, E., Niebuhr, K., Cabiaux, V., Parsot, C. & Sansonetti, P. (1999). The tripartite type III secreton of *Shigella flexneri* inserts IpaB and IpaC into host membranes. *J Cell Biol* **147**, 683-93.

3. Blocker, A., Jouihri, N., Larquet, E., Gounon, P., Ebel, F., Parsot, C., Sansonetti, P. & Allaoui, A. (2001). Structure and composition of the *Shigella flexneri* "needle complex", a part of its type III secreton. *Mol Microbiol* **39**, 652-63.

4. Marlovits, T. C., Kubori, T., Sukhan, A., Thomas, D. R., Galan, J. E. & Unger, V. M. (2004). Structural insights into the assembly of the type III secretion needle complex. *Science* **306**, 1040-2.

5. Morita-Ishihara, T., Ogawa, M., Sagara, H., Yoshida, M., Katayama, E. & Sasakawa, C. (2006). *Shigella* Spa33 is an essential C-ring component of type III secretion machinery. *J Biol Chem* **281**, 599-607.

6. Kubori, T., Matsushima, Y., Nakamura, D., Uralil, J., Lara-Tejero, M., Sukhan, A., Galan, J. E. & Aizawa, S. I. (1998). Supramolecular structure of the *Salmonella typhimurium* type III protein secretion system. *Science* **280**, 602-5.

7. Kubori, T. & Galan, J. E. (2002). *Salmonella* type III secretion-associated protein InvE controls translocation of effector proteins into host cells. *J Bacteriol* **184**, 4699-708.

8. Hoiczyk, E. & Blobel, G. (2001). Polymerization of a single protein of the pathogen *Yersinia enterocolitica* into needles punctures eukaryotic cells. *Proc Natl Acad Sci U S A* **98**, 4669-74.

9. Van Gijsegem, F., Vasse, J., Camus, J. C., Marenda, M. & Boucher, C. (2000). *Ralstonia solanacearum* produces hrp-dependent pili that are required for PopA secretion but not for attachment of bacteria to plant cells. *Mol Microbiol* **36**, 249-60.

10. Knutton, S., Rosenshine, I., Pallen, M. J., Nisan, I., Neves, B. C., Bain, C., Wolff, C., Dougan, G. & Frankel, G. (1998). A novel EspA-associated surface organelle of *enteropathogenic Escherichia* coli involved in protein translocation into epithelial cells. *Embo J* **17**, 2166-76.

11. Daniell, S. J., Takahashi, N., Wilson, R., Friedberg, D., Rosenshine, I., Booy, F. P., Shaw, R. K., Knutton, S., Frankel, G. & Aizawa, S. (2001). The filamentous type III secretion translocon of enteropathogenic *Escherichia coli*. *Cell Microbiol* **3**, 865-71.

12. Crepin, V. F., Shaw, R., Abe, C. M., Knutton, S. & Frankel, G. (2005). Polarity of enteropathogenic *Escherichia coli* EspA filament assembly and protein secretion. *J Bacteriol* **187**, 2881-9.

13. Mota, L. J. & Cornelis, G. R. (2005). The bacterial injection kit: type III secretion systems. *Ann Med* **37**, 234-49.

14. Cornelis, G. R. (2006). The type III secretion injectisome. *Nat Rev Microbiol* **4**, 811-25.

15. Michiels, T. & Cornelis, G. R. (1991). Secretion of hybrid proteins by the *Yersinia* Yop export system. *J Bacteriol* **173**, 1677-85.

16. Galan, J. E. & Wolf-Watz, H. (2006). Protein delivery into eukaryotic cells by type III secretion machines. *Nature* **444**, 567-73.

17. Journet, L., Agrain, C., Broz, P. & Cornelis, G. R. (2003). The needle length of bacterial injectisomes is determined by a molecular ruler. *Science* **302**, 1757-60.

18. Mueller, C. A., Broz, P., Muller, S. A., Ringler, P., Erne-Brand, F., Sorg, I., Kuhn, M., Engel, A. & Cornelis, G. R. (2005). The V-antigen of *Yersinia* forms a distinct structure at the tip of injectisome needles. *Science* **310**, 674-6.

19. Goure, J., Broz, P., Attree, O., Cornelis, G. R. & Attree, I. (2005). Protective anti-V antibodies inhibit *Pseudomonas* and *Yersinia* translocon assembly within host membranes. *J Infect Dis* **192**, 218-25.

20. Makishima, S., Komoriya, K., Yamaguchi, S. & Aizawa, S. I. (2001). Length of the flagellar hook and the capacity of the type III export apparatus. *Science* **291**, 2411-3.

21. Marlovits, T. C., Kubori, T., Lara-Tejero, M., Thomas, D., Unger, V. M. & Galan, J. E. (2006). Assembly of the inner rod determines needle length in the type III secretion injectisome. *Nature* **441**, 637-40.

22. Sorg, I., Wagner, S., Amstutz, M., Muller, S. A., Broz, P., Lussi, Y., Engel, A. & Cornelis, G. R. (2007). YscU recognizes translocators as export substrates of the *Yersinia* injectisome. *Embo J* **26**, 3015-24.

23. Agrain, C., Callebaut, I., Journet, L., Sorg, I., Paroz, C., Mota, L. J. & Cornelis, G. R. (2005). Characterization of a Type III secretion substrate specificity switch (T3S4) domain in YscP from *Yersinia enterocolitica. Mol Microbiol* **56**, 54-67.

24. Agrain, C., Sorg, I., Paroz, C. & Cornelis, G. R. (2005). Secretion of YscP from *Yersinia enterocolitica* is essential to control the length of the injectisome needle but not to change the type III secretion substrate specificity. *Mol Microbiol* **57**, 1415-27.

25. Allaoui, A., Woestyn, S., Sluiters, C. & Cornelis, G. R. (1994). YscU, a *Yersinia enterocolitica* inner membrane protein involved in Yop secretion. *J Bacteriol* **176**, 4534-42.

26. Minamino, T. & Macnab, R. M. (2000). Domain structure of *Salmonella* FlhB, a flagellar export component responsible for substrate specificity switching. *J Bacteriol* **182**, 4906-14.

27. Lavander, M., Sundberg, L., Edqvist, P. J., Lloyd, S. A., Wolf-Watz, H. & Forsberg, A. (2002). Proteolytic cleavage of the FlhB homologue YscU of *Yersinia pseudotuberculosis* is essential for bacterial survival but not for type III secretion. *J Bacteriol* **184**, 4500-9.

28. Zarivach, R., Deng, W., Vuckovic, M., Felise, H. B., Nguyen, H. V., Miller, S. I., Finlay, B. B. & Strynadka, N. C. (2008). Structural analysis of the essential self-cleaving type III secretion proteins EscU and SpaS. *Nature* **453**, 124-7.

29. Deane, J. E., Graham, S. C., Mitchell, E. P., Flot, D., Johnson, S. & Lea, S. M. (2008). Crystal structure of Spa40, the specificity switch for the *Shigella flexneri* type III secretion system. *Mol Microbiol*.

30. Bürgi, H. B., Dunitz, J.D., Shefter, E. (1973). Geometrical reaction coordinates. II. Nucleophilic addition to a carbonyl group. *J Am Chem Soc* **95**, 5065-5067.

31. Bürgi, H. B., Dunitz, J.D., Lehn, J.M. & Wipff, G. (1974). Stereochemistry of reaction paths at carbonyl centres. *Tetrahedron* **30**, 1563-1572.

32. Ferris, H. U., Furukawa, Y., Minamino, T., Kroetz, M. B., Kihara, M., Namba, K. & Macnab, R. M. (2005). FlhB regulates ordered export of flagellar components via autocleavage mechanism. *J Biol Chem* **280**, 41236-42.

33. Ding, Y., Xu, M. Q., Ghosh, I., Chen, X., Ferrandon, S., Lesage, G. & Rao, Z. (2003). Crystal structure of a mini-intein reveals a conserved catalytic module involved in side chain cyclization of asparagine during protein splicing. *J Biol Chem* **278**, 39133-42.

34. Gunasekaran, K., Ramakrishnan, C. & Balaram, P. (1997). Beta-hairpins in proteins revisited: lessons for de novo design. *Protein Eng* **10**, 1131-41.

35. Wood, S. E., Jin, J. & Lloyd, S. A. (2008). YscP and YscU switch the substrate specificity of the *Yersinia* type III secretion system by regulating export of the inner rod protein YscI. *J Bacteriol* **190**, 4252-62.

36. Riordan, K. E. & Schneewind, O. (2008). YscU cleavage and the assembly of *Yersinia* type III secretion machine complexes. *Mol Microbiol* **68**, 1485-501.

37. Fraser, G. M., Hirano, T., Ferris, H. U., Devgan, L. L., Kihara, M. & Macnab, R. M. (2003). Substrate specificity of type III flagellar protein export in *Salmonella* is controlled by subdomain interactions in FlhB. *Mol Microbiol* **48**, 1043-57.

38. Cornelis, G., Vanootegem, J. C. & Sluiters, C. (1987). Transcription of the yop regulon from *Y. enterocolitica* requires trans acting pYV and chromosomal genes. *Microb Pathog* **2**, 367-79.

39. Guerrero, S. A., Hecht, H. J., Hofmann, B., Biebl, H. & Singh, M. (2001). Production of selenomethionine-labelled proteins using simplified culture conditions and generally applicable host/vector systems. *Appl Microbiol Biotechnol* **56**, 718-23.

40. Otwinowski, Z. M., W. (1997). Processing of X-ray diffraction data collected in oscillation mode. *Methods Enzymol.* **276**, 307-326.

41. Leslie, A. G. (2006).The integration of macromolecular diffrection data. *Acta Crystallogr., D Biol. Crystalogr.* **62**, 48-57.

42. Panjikar, S., Parthasarathy, V., Lamzin, V. S., Weiss, M. S. & Tucker, P. A. (2005). Auto-Rickshaw: an automated crystal structure determination platform as an efficient tool for the validation of an X-ray diffraction experiment. *Acta Crystallogr D Biol Crystallogr* **61**, 449-57.

43. Emsley, P. & Cowtan, K. (2004). Coot: model-building tools for molecular graphics. *Acta Crystallogr D Biol Crystallogr* **60**, 2126-32.

44. Murshudov, G. N., Vagin, A. A. & Dodson, E. J. (1997). Refinement of macromolecular structures by the maximum-likelihood method. *Acta Crystallogr D Biol Crystallogr* **53**, 240-55.

45. Evans, P. (2006). Scaling and assessment of data quality. *Acta Crystallogr D Biol Crystallogr* **62**, 72-82.

46. McCoy, A. J., Grosse-Kunstleve, R. W., Storoni, L. C. & Read, R. J. (2005). Likelihood-enhanced fast translation functions. *Acta Crystallogr D Biol Crystallogr* **61**, 458-64.

47. Davis, I. W., Leaver-Fay, A., Chen, V. B., Block, J. N., Kapral, G. J., Wang, X., Murray, L. W., Arendall, W. B., 3rd, Snoeyink, J., Richardson, J. S. & Richardson, D. C. (2007). MolProbity: all-atom contacts and structure validation for proteins and nucleic acids. *Nucleic Acids Res* **35**, W375-83.

48. Guntert, P., Dotsch, V., Wider, G. & Wuthrich, K. (1992). Processing of Multidimensional Nmr Data with the New Software Prosa. *Journal of Biomolecular Nmr* **2**, 619-629.

49. Keller, R. (2004). Optimizing the process of NMR spectrum analysis and computer aided resonance assignment, ETH Zürich.

Figure Legends

Fig. 1. Ribbon plot of the monomer of YscU^{C} N263A. The position of the mutation in the cleavage site is indicated by an asterisk (*). After cleavage YscU^{C} is divided into an N-terminal and a C-terminal half, shown in brown and green, respectively. The modified NPTH motif, as well as Arg314 and Arg296, are depicted as stick-and-ball models.

Fig. 2. (a) Detailed stereoview of the modified NPTH motif of YscU^{C} N263D. The C-terminal and N-terminal halves are shown in brown and green respectively. The isosteric Asp263 is optimally positioned (109°) for a nucleophilic attack, as indicated by the red dashed line. Hydrogen bonds are indicated by black dashed lines. The ($2F_O$-F_C,α_C) electron density map of the cleavage site is depicted at a contour level of 1.5 σ.

(b) Orbital-model illustrating the stabilizing orbital overlap. The anti-bonding σ*-molecular orbital (MO) of the C_α-N bond in Asn263 (blue) interferes with the nascent bonding σ-MO of the C(=O)-N-bond (red).

Fig. 3. [^{15}N,^{1}H]-HMQC NMR spectra of YscU^{C}. The contour lines of wild-type YscU^{C} are shown in orange, those of YscU^{C} N263A in black.

Fig. 4. Cleveage behaviour of different YscU^{C} variants expressed in *E.coli*. (a) Coomassie-stained 15% SDS-PAGE analysis of cells producing various YscU^{C} variants. (b) Overexpressed cells analyzed by immunoblotting using an anti-YscU^{C} antibody. (c) pH-dependent cleavage of YscU^{C}-variants. SDS-PAGE analysis of purified YscU^{C}-variants incubated at different pH-values.

Fig. 5. Analysis of LcrV secretion by different *yscU* mutants. Total cell (TC) and supernatant (SN) fractions of corresponding in *trans* complemented *Yersinia* Δ*yscU* mutant bacteria analyzed by immunoblot with anti-LcrV antibodies.

Fig. 6. Needle length measurements of *yscU* mutant bacteria expressing the corresponding yscU alleles *in trans* from the pBAD promoter. Indicated are the median, the standard deviation (sd), and the number of needles measured (N).

Fig. 7. Structure-based model of succinimide-mediated cleavage of YscU. (I) His266 (or a His266-activated water molecule) abstracts a proton from the β-amide nitrogen of Asn262. The latter nucleophilically attacks the Asn262 carbonyl resulting in the rate-limiting tetrahedral intermediate (II). Cleavage of the peptide bond yields a labile C-terminal succinimide (III) which is hydrolysed to asparagine or iso-asparagine.

Fig. 8 (a) Structure-based sequence alignment of $YscU^C$ from *Y. enterocolitica* (Swiss-Prot. accession number Q56844) with $FlhB^C$ from *S. thyphimurium* (P40727), $EscU^C$ from *E. coli* (Q7DB59), $SpaS^C$ from *S. thyphimurium* (P40702), $Spa40^C$ from *S. flexneri* (Q6XVW1) and $HcrU^C$ from *X. oryzae* (Q5H6T1). The secondary structures are from $YscU^C$ N263D. Conserved amino acids are marked in bold letters on coloured backgrounds. Substituted residues in this study are indicated by a yellow background. Less conserved amino acids are also bold and coloured in blue.
(b) Stereoview $YscU^C$ variant N263D (green) superimposed on its wild-type homologues $EscU^C$ (blue), SpaSC (grey) and $Spa40^C$ (orange). Important positions are marked by a green sphere.

Fig. 9 Model of tripartite domain arrangement of YscU: The N-terminal, membrane-spanning domain is followed by a flexible linker region and a globular autocleavage domain.

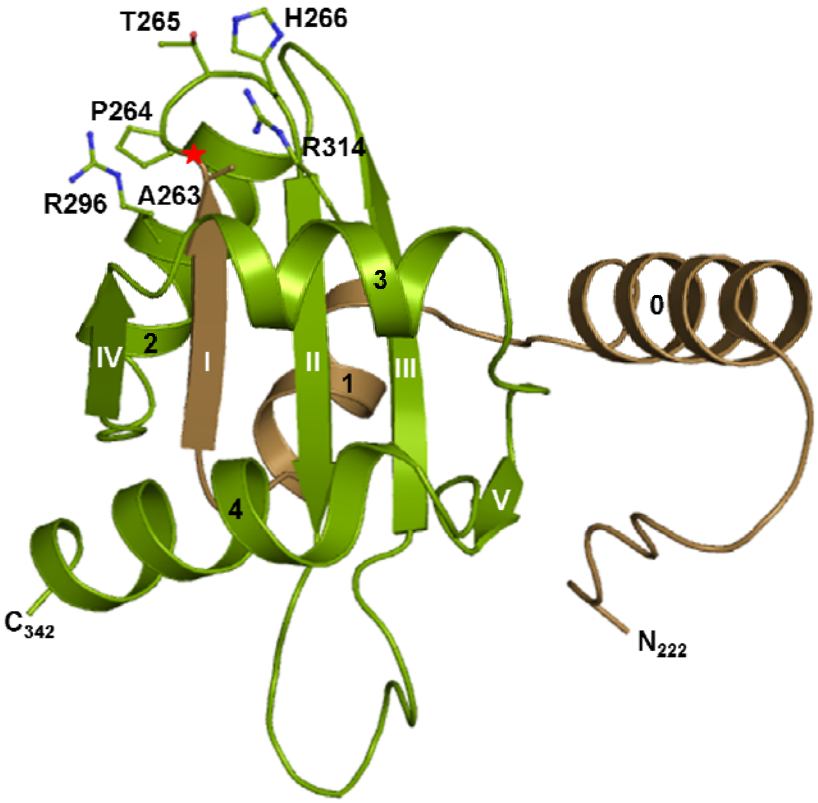

Figure 1 **Wiesand *et al.***

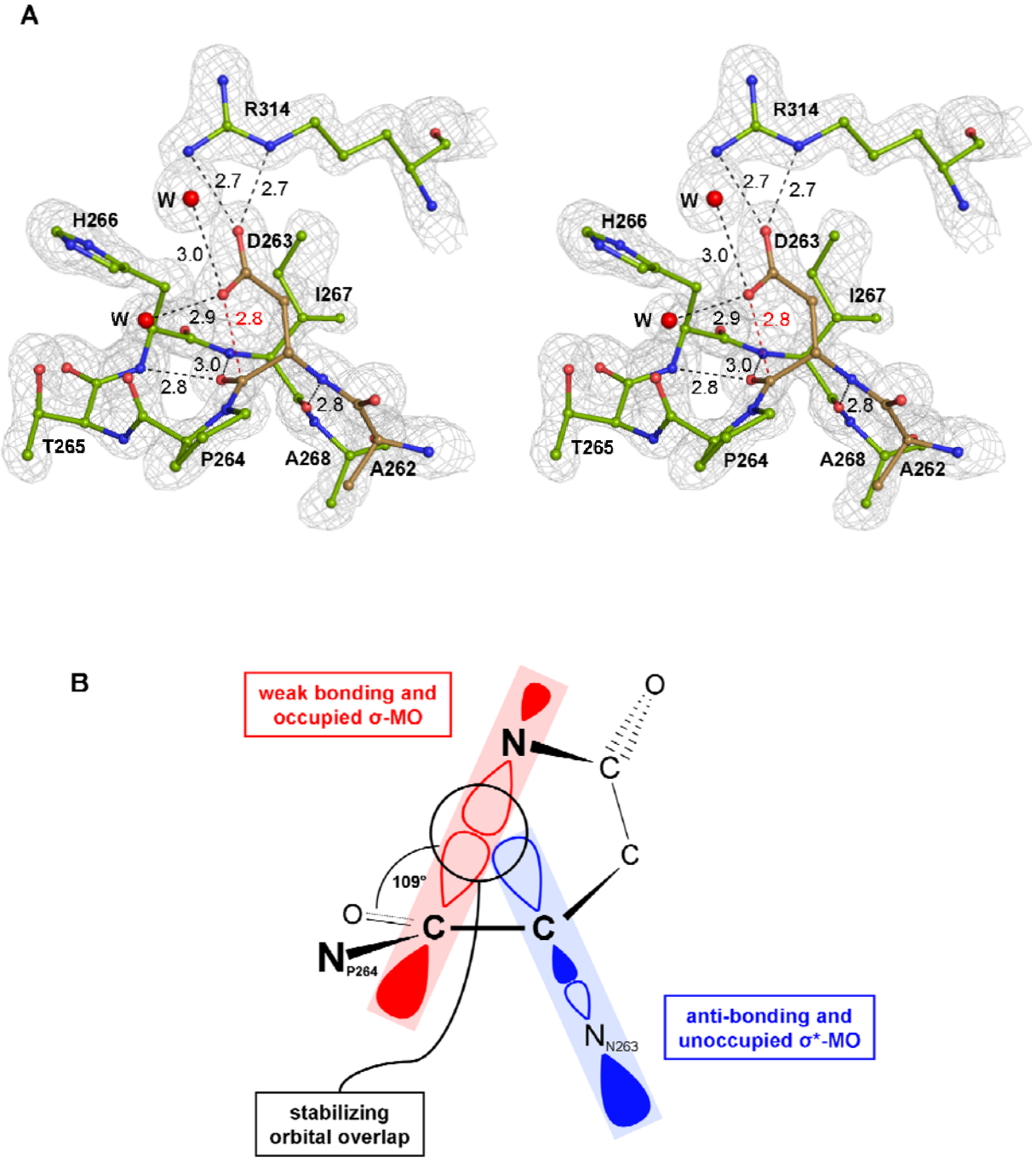

Figure 2 Wiesand *et al.*

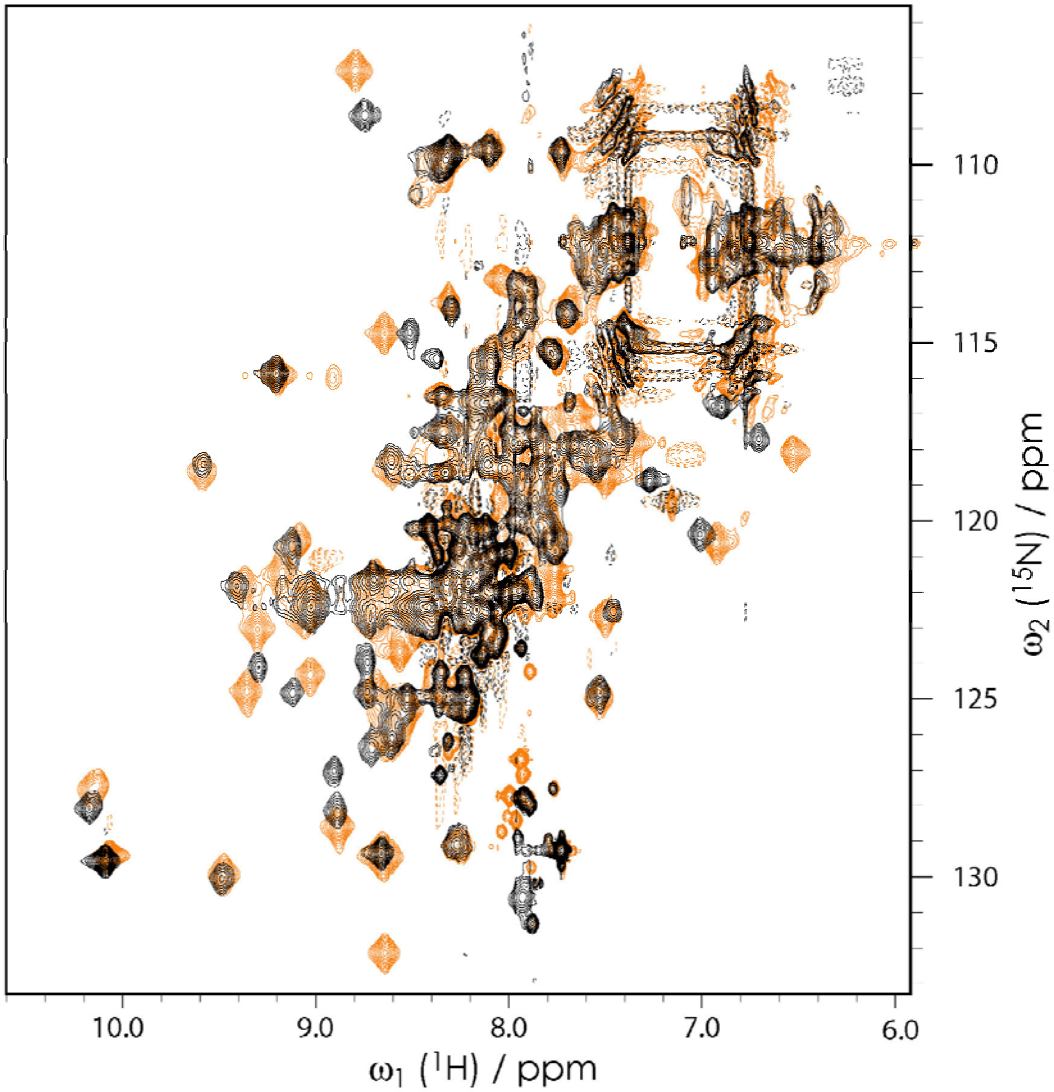

Figure 3 **Wiesand *et al.***

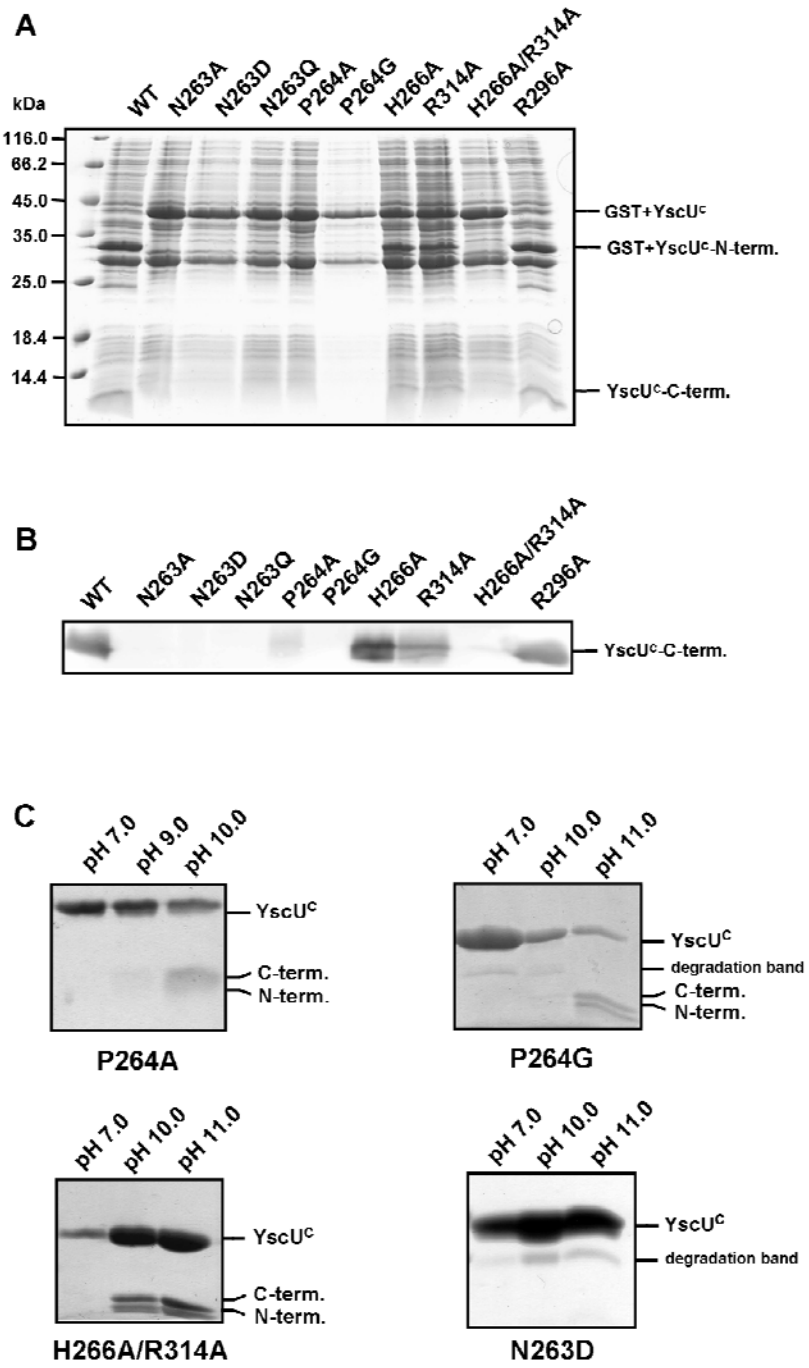

Figure 4 **Wiesand *et al.***

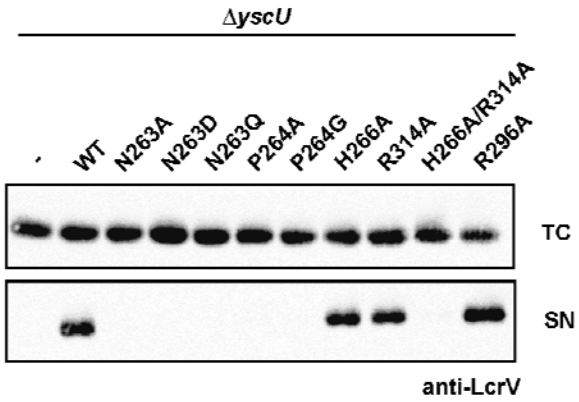

Figure 5 Wiesand *et al.*

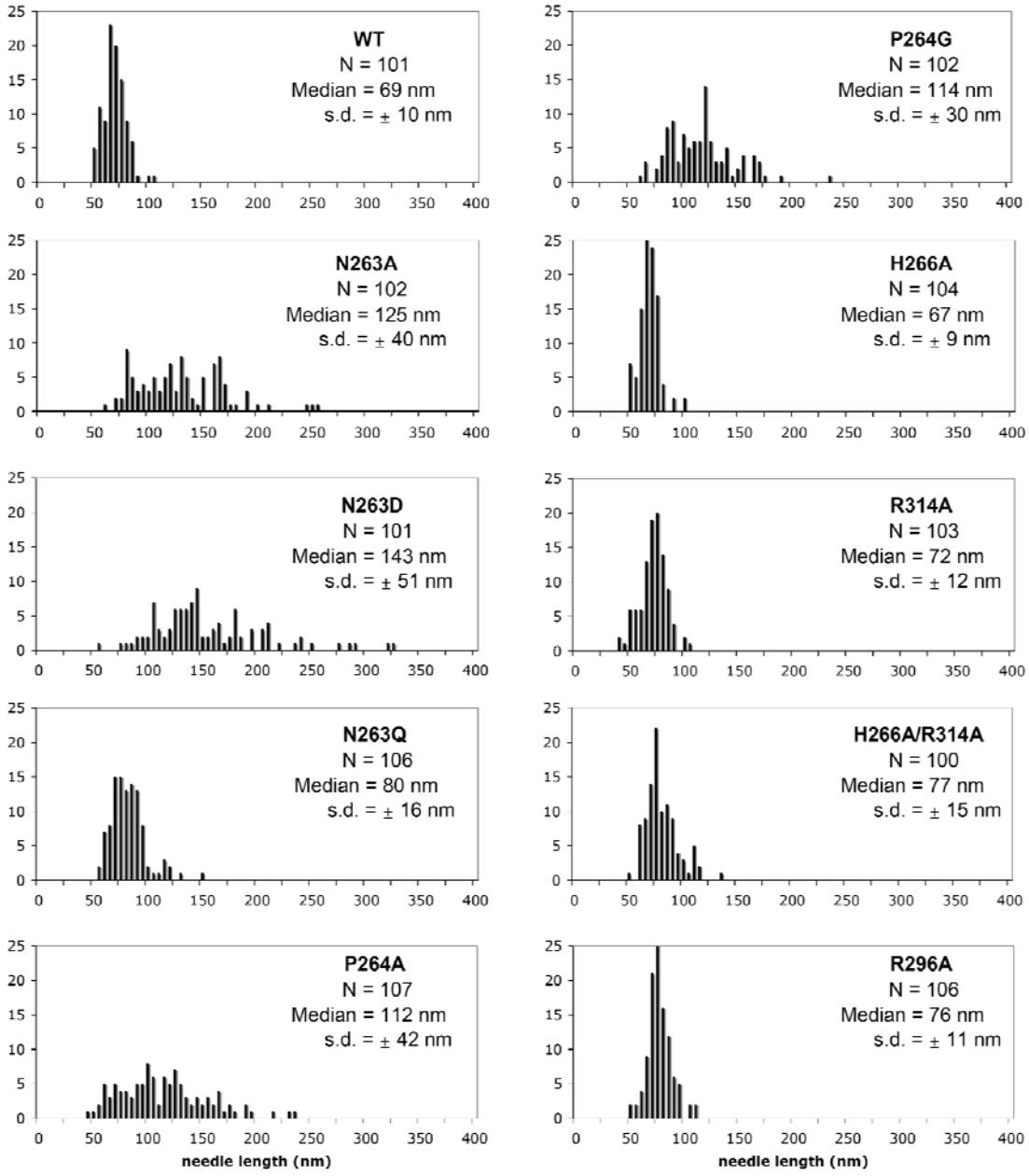

Figure 6 Wiesand *et al.*

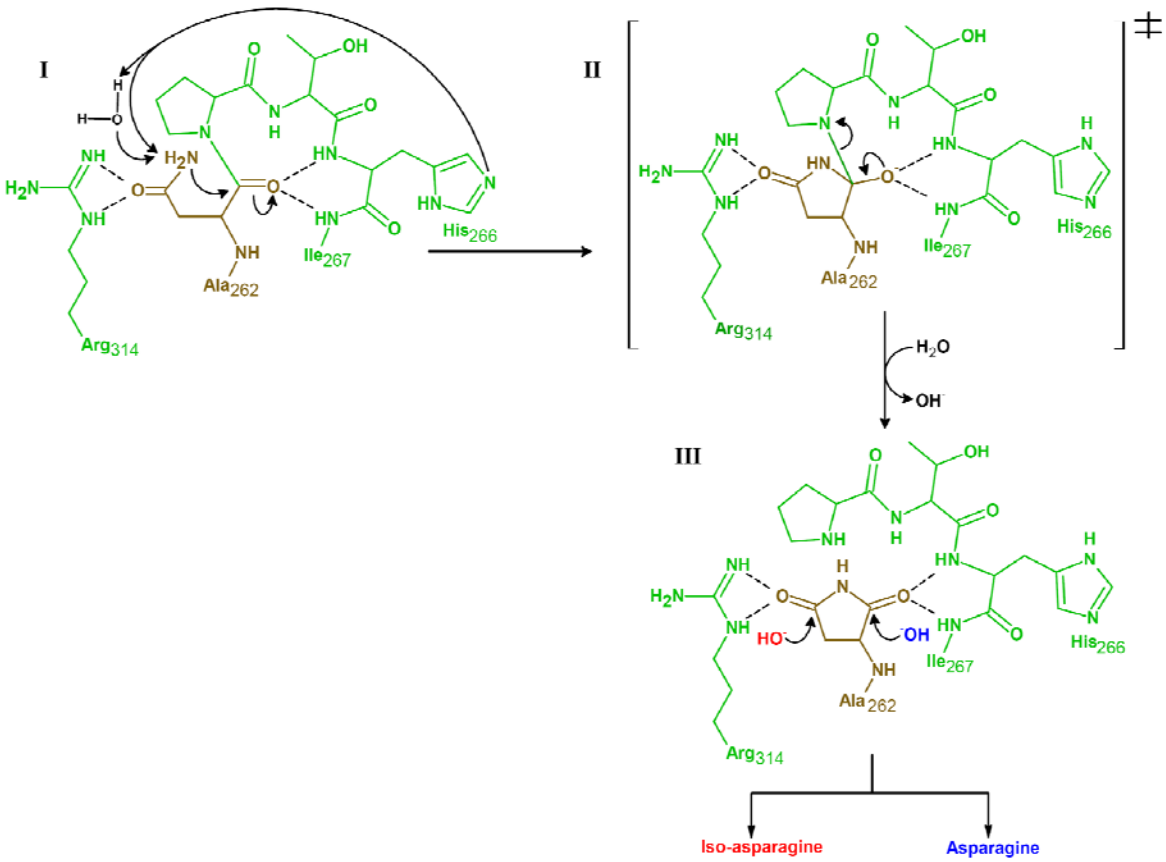

Figure 7 **Wiesand *et al.***

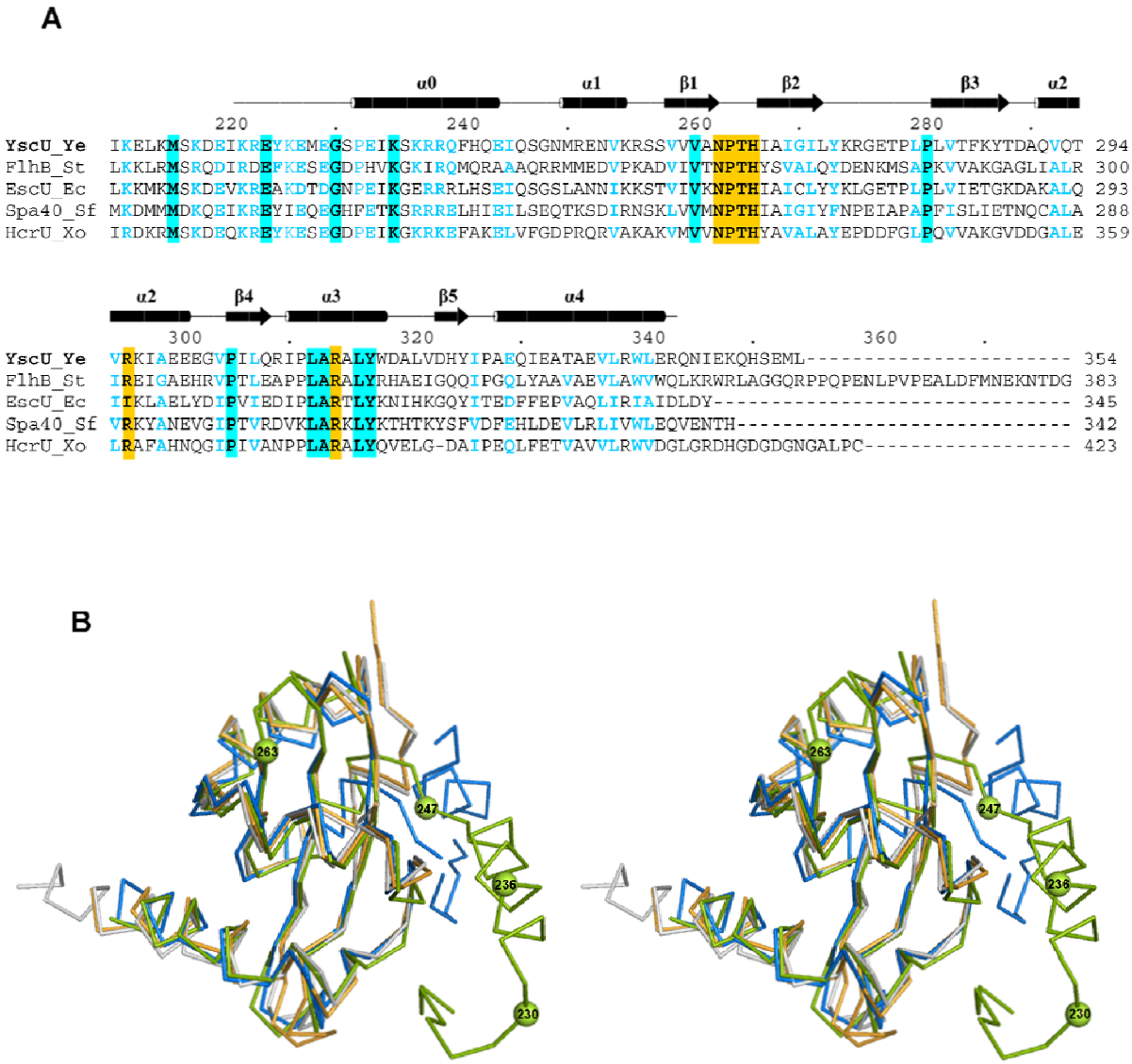

Figure 8 **Wiesand *et al.***

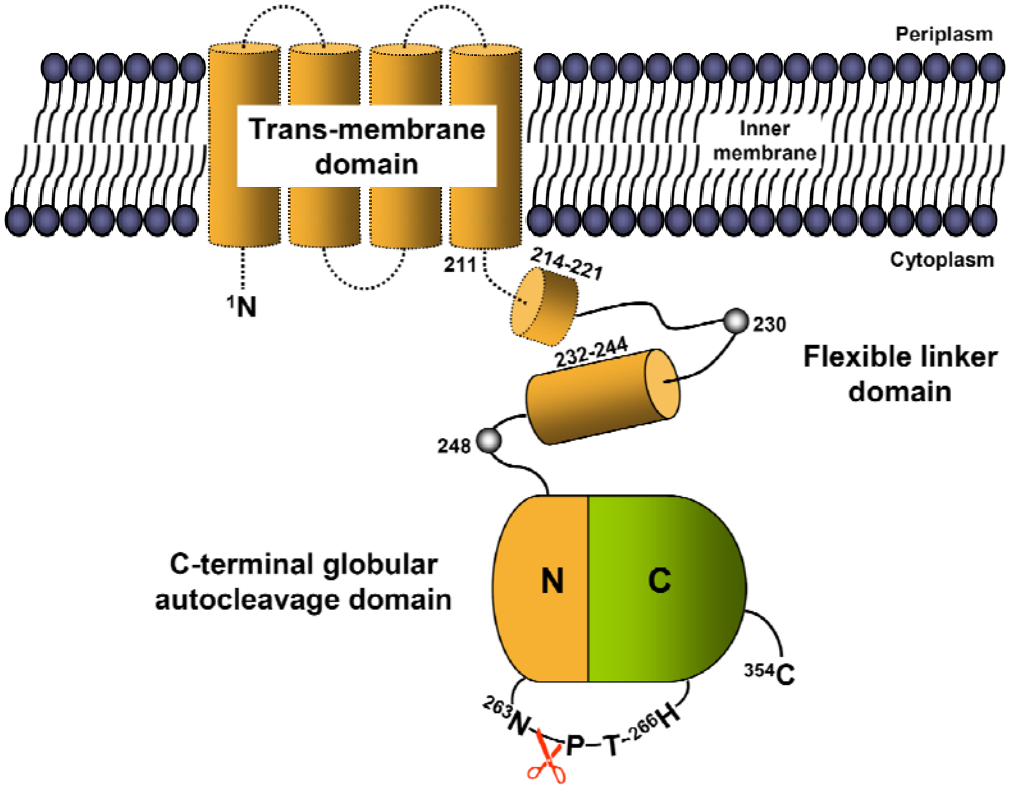

Figure 9 Wiesand *et al.*

Table 1 Data collection and refinement statistics

	SeMet-labeled YscU^{N263A}				YscU^{N263D}
	Peak	Inflection	High remote	Low remote	
Data collection ststistics					
Beamline	DESY X12	DESY X12	DESY X12	DESY X12	ESRF ID29
Space group	$P4_32_12$	$P4_32_12$	$P4_32_12$	$P4_32_12$	$P4_32_12$
Unit cell: a, c (Å)	66.2, 68.1	66.2, 68.1	66.2, 68.1	66.3, 68.8	66.5, 68.1
Wavelength (A)	0.97854	0.97893	0.95370	1.0000	0.9500
Resolution (A)	30.0-2.33 (2.41-2.33)	40.0-2.33 (2.41-2.33)	40.0-2.33 (2.41-2.33)	30.0-2.0 (2.11-2.0)	10.0-1.55 (1.63-1.55)
Mosaicity (°)	0.80	0.98	0.89	0.95	0.24
Unique reflections	6910 (670)	6907 (663)	6920 (667)	10836 (1517)	21871 (3232)
Completeness (%)	100 (99.9)	100 (100)	100 (100)	100 (100)	96.7 (99.9)
Multiplicity	13.6 (12.0)	13.6 (12.6)	13.8 (13.3)	13.6 (13.6)	3.1 (3.1)
I/σ_I	31.7 (8.2)	34.3 (8.8)	34.0 (9.5)	8.1 (2.2)	8.4 (4.8)
R_{merge}(%)[a]	8.2 (31.5)	7.7 (29.8)	7.8 (31.0)	6.9 (35.2)	5.2 (15.1)
Wilson B-factor (Å^2)	39	39	38	25	19
Solvent content (%)	45	45	45	45	45
Refinament statistics					
R_{cryst}/R_{free}[b] (%)				22.1 / 25.3	20.1 / 22.5
Number of atoms Protein / solvent / chloride				1027 / 52 / 1	1104 / 133 / 2
r.m.s.d. Bonds (Å) / angle (°)				0.015 / 1.756	0.019 / 1.698
Ramachandran plot					
Residues in favoured / Allowed regions (%)				95.3 / 4.7	96.4 / 3.6
B-factor (Å^2) average Protein / solvent / chloride				29.9 / 34.7 / 27.0	20.3 / 33.6 / 35.1

Values in parentheses refer to the highest resolution shell.

[a] $R_{merge} = 100\ \Sigma_n\left(\Sigma_i\left|I_i - \bar{I}\right|\right)/\Sigma_n\left(\Sigma I_i\right)$

[b] $R_{cryst} = 100\ \Sigma_{hkl}\left|F_o - F_c\right|/\Sigma_{hkl} F_o$. Test set size for YscU^{N203A} Irem 5% and for YscU^{N203D} 3%.

Supplement 1 Plasmids used in this work

Plasmids	Current strain designation	Genotype and derivation	References
pYV plasmids			
pYV40	WT	pYV plasmid from *Y. enterocolitica* E40	Sory *et al.*[1]
pYVe22703	pYVe22703	pYV plasmid from *Y. enterocolitica* W227 serotype O:9	Cornelis *et al.*[2]
pLY4001	Δ*yscU*	pYV40 Δ*yscU;* deletion of yscU codons 1-354	Sorg *et al.*[3]
Expression plasmids			
pBADMycHisA			Invitrogen
pLY7	*yscU*$^{+++}$	pBAD:: *yscU*; *yscU* was amplified from pYVe22703 using oligos 3704 and 3724 and cloned into the *NcoI* / *EcoRI* sites of pBADmycHisA	Sorg *et al.*[3]
pSTW7	$yscU_{N263A}{}^{+++}$	pBAD:: $yscU_{N263A}$; mutation N263A was introduced into pLY7 by site directed mutagenesis using oligos 3725 and 3726	Sorg *et al.*[3]
pISO153	$yscU_{R314A}{}^{+++}$	pBAD:: $yscU_{R314A}$; mutation R314A was introduced into pLY7 by site directed mutagenesis using oligos 4842 and 4843	this study
pISO166	$yscU_{N263D}{}^{+++}$	pBAD:: $yscU_{N263D}$; mutation N263D was introduced into pLY7 by overlapping PCR using oligos 3724/4955 and 4954/3704	this study
pISO167	$yscU_{N263Q}{}^{+++}$	pBAD:: $yscU_{N263Q}$; mutation N263Q was introduced into pLY7 by overlapping PCR using oligos 3724/4957 and 4956/3704	this study
pISO168	$yscU_{H266A}{}^{+++}$	pBAD:: $yscU_{H266A}$; mutation H266A was introduced into pLY7 by overlapping PCR using oligos 3724/4959 and 4958/3704	this study
pISO169	$yscU_{H266A/R314A}{}^{+++}$	pBAD:: $yscU_{H266A/R314A}$; mutation H266A was introduced into pISO153 by overlapping PCR using oligos 3724/4959 and 4958/3704	this study
pISOA174	$yscU_{P264G}{}^{+++}$	pBAD:: $yscU_{P264G}$; mutation P264G was introduced into pLY7 by site directed mutagenesis using oligos 5031 and 5032	this study
pISOA175	$yscU_{R296A}{}^{+++}$	pBAD:: $yscU_{R296A}$; mutation R296A was introduced into pLY7 by site directed mutagenesis using oligos 5033 and 5034	this study

[1]Sory MP, Boland A, Lambermont I, Cornelis GR (1995) Identification of the YopE and YopH domains required for secretion and internalization into the cytosol of macrophages, using the cyaA gene fusion approach. *Proc Natl Acad Sci U S A* **92:** 11998-12002.
[2]Cornelis G, Vanootegem JC, Sluiters C (1987) Transcription of the yop regulon from Y. enterocolitica requires trans acting pYV and chromosomal genes. *Microb Pathog* **2:** 367-379.
[3]Sorg, I., Wagner, S., Amstutz, M., Muller, S. A., Broz, P., Lussi, Y., Engel, A. & Cornelis, G. R. (2007). YscU recognizes translocators as export substrates of the Yersinia injectisome. *Embo J* **26**, 3015-24.

Supplement 2 Oligonucleotides used for the genetic constructions

No.	Sequence	Restriction site
3704	gatcgaattcttataacatttcggaatg	*EcoRI*
3724	gatcccatggccagcggagaaaagacagag	*NcoI*
4842	atcccattagccgctgctctttattgg	
4843	ccaataaagagcagcggctaatgggat	
4956	gtggtggtagctcagccgacccatattg	
4957	caatatgggtcggctgagctaccaccac	
4958	gctaatccgaccgctattgctattgg	
4959	ccaatagcaatagcggtcggattagc	
5031	gctcatcagtggtggtagctaatgggacccatattgctattggtattctttataagc	
5032	gcttataaagaataccaatagcaatatgggtcccattagctaccaccactgatgagc	
5033	cgatgcccaagttcagactgtggccaaaatagcagaagaagaagg	
5034	ccttcttcttctgctattttggccacagtctgaacttgggcatcg	